

Article

Lipid Differences and Related Metabolism Present on the Hand Skin Surface of Different-Aged Asiatic Females—An Untargeted Metabolomics Study

Tian Chen ^{1,2}, Juan Wang ³ and Zhenxing Mao ^{3,*}¹ Division of Public Health Service and Safety Assessment,

Shanghai Municipal Center for Disease Control and Prevention, Shanghai 200336, China

² NMPA Key Laboratory for Monitoring and Evaluation of Cosmetics, Shanghai 200336, China³ College of Public Health, Zhengzhou University, Zhengzhou 450001, China

* Correspondence: mzx@zzu.edu.cn; Tel.: +86-371-67781452; Fax: +86-371-67781868

Abstract: This cross-sectional study aimed to investigate differences in skin surface lipids (SSL) and explore related metabolic pathways among females of different ages in Henan Province. Ultra-performance liquid chromatography quadrupole time-of-flight mass spectrometry (UPLC-QTOF-MS) was used to determine the lipid composition of the skin surface of 58 female volunteers who were divided into three age groups. Statistical analysis was performed using Progenesis QI, Ezinfo, and MetaboAnalyst. Multivariate and enrichment analysis were used to identify the different SSL among the groups. A total of 530 lipid entities were identified and classified into eight classes. Among these, 63 lipids were significantly different between the groups. Lower levels of glycerolipids (GLs) and sphingolipids (SPs) were observed in the middle-aged group, while higher levels of GLs were found in the elder group. GLs belonged to the largest and statistically significant enrichment of lipid metabolic pathways, and the lipid individuals enriched to the sphingoid bases metabolism were the most and statistically significant. These findings suggest that there are differences in hand SSL among females of different ages, which may be related to GLs and sphingoid bases metabolism.

Keywords: skin surface lipids; lipidomic analysis; female hand



Citation: Chen, T.; Wang, J.; Mao, Z. Lipid Differences and Related Metabolism Present on the Hand Skin Surface of Different-Aged Asiatic Females—An Untargeted Metabolomics Study. *Metabolites* **2023**, *13*, 553. <https://doi.org/10.3390/metabo13040553>

Academic Editor: Zhuzhen Zhang

Received: 9 February 2023

Revised: 23 March 2023

Accepted: 25 March 2023

Published: 13 April 2023



Copyright: © 2023 by the authors. Licensee MDPI, Basel, Switzerland. This article is an open access article distributed under the terms and conditions of the Creative Commons Attribution (CC BY) license (<https://creativecommons.org/licenses/by/4.0/>).

1. Introduction

The skin is the largest and outermost organ of the human body and has a variety of defense and regulatory functions [1]. The stratum corneum (SC), formed by terminally differentiated keratinocytes in the outermost layer of the epidermis, mainly provides the skin surface barrier function [2]. The skin surface barrier is composed of a “brick–mortar” structure, where the “bricks” are non-nucleated stratum corneum cells, and the “mortar” is a lipid-rich extracellular matrix [3,4]. The lipids on the skin surface, composed of ceramides, cholesterol, free fatty acids (FAs), and some small molecular lipids, play a crucial role in maintaining the skin barrier function [5]. These lipids are derived from precursor cells and are then “lipid processed” by enzymes released from the epidermal lamellar bodies into intercellular lipids [6]. Any factor that affects the skin surface acidity, Ca⁺ concentration gradient, and barrier function can impact lipid turnover [7].

The natural aging process of the skin leads to a loss of elasticity, dryness, fine lines, atrophy, and laxity of the skin. The two main mechanisms responsible for these changes are intrinsic aging and environment-dependent extrinsic aging, caused by exposure to sunlight-related UV radiation (photoaging), smoking, and air pollution, among others [8,9]. The stratum corneum’s barrier function is also incapable of resisting the aging process, and age-related skin changes can lead to visible signs of aging and structural and functional impairments [10]. A damaged epidermal permeability barrier (EPB) leads to transepidermal water loss (TEWL) and triggers inflammatory skin diseases that negatively impact the

quality of life [11]. Many skin diseases, such as lamellar ichthyosis, psoriasis, Netherton syndrome (NTS), and atopic dermatitis (AD), are characterized by defective or weakened epidermal barrier function [12]. In addition, the prevention of skin aging and skin rejuvenation are becoming areas of active research. Aging is inherently complex, and it is difficult to quantify and interpret experimental results. Previous studies on changes in barrier function with age have been controversial. Therefore, new technology is needed to explore the damage mechanism of skin barrier function with age. This will enable us to quantify the degree of damage and provide a theoretical basis for the development and optimization of corresponding skin care products.

Lipidomics is a powerful analytical tool that utilizes liquid chromatography–mass spectrometry (LC–MS) machines to study human lipid metabolites through the principles of analytical chemistry [13]. It is widely used in various fields, including cancer [14], metabolic syndrome [15], and skin diseases [16] due to its ability to evaluate all lipids in biological systems and conduct large-scale lipid research [13]. By analyzing and identifying lipid differences between different populations, lipidomics can help explore differential pathways of lipid metabolism, which provides a basis for studying the pathogenesis of diseases. Previous studies have investigated the characteristics of skin aging by distinguishing between parts of the skin that are subjected or not to sunlight. In particular, facial skin has been actively studied because it is not only the part that is exposed to the outside world, but it is also the part of the body that attracts more aesthetic attention than other parts of the body [17]. Conversely, limited research has been conducted on hand skin, despite the fact that it is also exposed and is the most vulnerable structure besides the head to environmental stresses (abrasions, cuts, lacerations, and chemical and thermal burns). In addition, unlike the skin on the surface of the hand and palm, the skin on the back of the hand has relatively abundant sebaceous glands [18]. The skin on the back of the hand was selected as a sampling point for this study. Meanwhile, gender differences in skin have to be considered [19]. Compared with males, females in rural China are generally more likely to engage in domestic work and to be exposed to detergents or solid particles associated with cooking [20,21]. Therefore, a cross-sectional study was conducted, which recruited a group of healthy female subjects of different ages. Non-invasive skin detection technology and lipidomics were used to evaluate the skin barrier function of people of different ages and explore the related metabolic pathways.

2. Materials and Methods

2.1. Chemicals and Reagents

LC–MS-grade acetonitrile (ACN, catalog no. A955-4), methanol (MT, catalog no. A456-4), ammonium formate (catalog no. A115-50), isopropyl alcohol (IPA, catalog no. A461-4), N-propanol (NPA, catalog no. A414-4), acetonitrile (catalog no. A955-4), and formic acid (catalog no. LS118-4) were obtained from Thermo Fisher (Waltham, MA, USA). skin surface lipids (SSL)-adsorbent tapes Corneofix[®] (Cologne, Germany) and a Mass Spectrometer (Waters UPLC-VION QTOF MS, Milford, MA, USA) were used for this study.

2.2. Study Participants

Female volunteers aged 18 to 79 years from rural Henan, China, were recruited for the study. The inclusion criteria were as follows: (a) healthy volunteers aged 18–79 years, who were divided into a younger group: 18–44 years old, middle-aged group: 45–59 years old, and elder group: 60–79 years old; (b) no previous common skin diseases, such as contact dermatitis, eczema, urticaria, etc.; (c) refrain from using any skincare or washing products for at least 3 days before testing; (d) do not smoke, drink, or stay up late. (e) do not spend more than 4 h outdoors every day. The exclusion criteria included: (a) not persisting until the end of the experiment; (b) sensitive skin. Due to age differences in the biophysical characteristics of skin, in this study, according to the guidance of WHO and the actual situation in our country, the subjects were divided into three age groups to analyze the changes in SSL [22]. Finally, a total of 58 subjects were enrolled in the study. All participants

were informed about the study's purpose and methods and signed a written informed consent form. The study was conducted with the approval of the Ethics Committee of Zhengzhou University and conforms to the principles of the Declaration of Helsinki.

2.3. Sample Collection and Preparation

The collection of skin lipid samples was performed in May 2020. Before collecting samples, the righthand surface was cleaned with clean water and dried with a non-woven fabric. After sitting indoors for 30 min (the temperature was kept at 20 ± 1 °C, and the relative humidity was about 40–60 %), the experimenter attached the Corneofix[®] test strips to the back of the volunteer's right hand. The strips were removed after 30 min, placed in 2 mL EP tubes, and stored frozen at -80 °C.

For preparation, the samples were retrieved from the freezer, and 1.5 mL of methanol was added; then, they were vortexed for 60 min and allowed to settle at -20 °C for 12 h. The Corneofix[®] test strips were retrieved from the EP tubes, and the remaining lipid-containing extract was blow-dried using the nitrogen evaporator (Hengao, China). Finally, the residue was redissolved in 200 μ L of IPA/ACN/distilled water (65/30/5) and transferred to a vial for detection after vortexing.

2.4. Ultraperformance Liquid Chromatography Analysis

Chromatographic separation (Waters, USA) was performed on an ACQUITY UPLC CSH C18-column, 2.1×100 mm, 1.7 μ m particle size. The flow rate was set at 0.3 mL/min, the column temperature was kept at 50 °C, and the sample injection volume was 5 μ L. Mobile phase A was composed of a solution of 10 mM ammonium formate with 0.1% formic acid in ACN/water (60:40, *v/v*), while mobile phase B was composed of a solution of 0.1% formic acid in IPA/ACN (90:10, *v/v*). Gradient elution was performed with a mixture of mobile phase A and mobile phase B (details provided in Table 1).

Table 1. The gradient conditions of mobile phases.

Time (min)	A Phase (%)	B Phase (%)
0.0	80	20
1.0	80	20
5.0	40	60
11.0	20	80
18.0	10	90
19.0	0	100
21.0	0	100
21.1	80	20
22.0	80	20

2.5. Mass Spectrometry Analysis

Mass spectra were generated by electrospray ionization (ESI) in the positive mode, with a range of *m/z* 50 to 1000 for scanning. Data acquisition was performed using MSE in the continuum mode, with leucine enkephalin (*m/z* 554.2771) as the lock mass for mass correction. In the positive ion mode, the capillary voltage was set to 3000 V, the source temperature was set to 120 °C, and the desolvation temperature was set to 500 °C. The cone gas and desolvation flow rate were 50 L/h and 900 L/h, respectively (see Supplementary Table S1).

2.6. Data Extraction and Analysis

First, all mass spectral data of the samples were imported into Progenesis QI 3.0.3 (Waters Corporation) for data processing, including peak alignment, peak extraction, normalization, etc. The Lipid Maps Structure Database (LMSD) (<http://www.lipidmaps.org>, accessed on 15 August 2022) and the human metabolome database (HMDB) (<https://hmdb.ca/>, accessed on 16 August 2022) were performed to identify the compound ID of the lipid composition of each sample. Second, lipid composition data were imported into MetaboAnalyst 5.0 (<https://dev.metaboanalyst.ca/>, accessed on 29 August 2022) to explore the distribution of SSL between the three groups by heatmaps. Third, the preprocessed data imported into QI were grouped into three groups and then imported into Ezinfo (Waters Corporation) for analysis. Principal component analysis (PCA) and supervised partial least-squares discriminant analysis (PLS-DA) were performed to visualize the metabolic and lipid differences between the groups. The corresponding loading plot was used to determine the metabolites most responsible for separation in the PLS-DA model. Based on these results, important differential metabolites were evaluated by the values of variable importance in the projection (VIP), fold change (FC) and p -value, with the criteria of simultaneously meeting $VIP > 1$, $|FC| \geq 2$, and $p\text{-value} < 0.05$. In addition, significant differences between relative abundances in groups were assessed with the one-way Analysis of Variance (ANOVA) with SPSS software version 21.0, and a two-tailed $p < 0.05$ was considered statistically significant. Finally, we used metabolite set enrichment analysis (MSEA) to investigate lipid metabolism pathways that were enriched by differentiated lipids in MetaboAnalyst.

3. Results

3.1. Differences in Right-Hand SSL in Females of Different Age Groups

The number of subjects in the three groups was 20 in the younger group, 19 in the middle-aged group, and 19 in the elder group. The age distribution of the participants was presented as the median (mean) respectively: 32.5 (33.4) y; 55 (51.9) y; and 66.5 (66.8) y. The 530 lipid entities were identified in the righthand SSL in three groups. A heat map was used to show the distribution of SSL at different ages of females. As shown in Figure 1a, the top 30 substances were singled out for display according to VIP. There was a significant separation of three groups, explaining that there were differences in right-hand SSL among them. Then, all identified lipids were classified into eight different classes. The relative content of each major lipid was calculated to compare the differences in lipids in females of different ages. Compared with the younger group, Figure 1b illustrated that the sterol lipids (STs) significantly decreased and the other lipids increased, including sphingolipids (SPs), prenol lipids (PRs), polyketides (PKs), and FAs, in the middle-aged group. Moreover, SPs and glycerolipids (GLs) increased significantly in the elderly group, while STs decreased ($p < 0.05$). It is worth noting that the pattern of expression of GLs and SPs seems to indicate that the younger group expresses fewer of these lipid types than the two older groups (all $p < 0.05$).

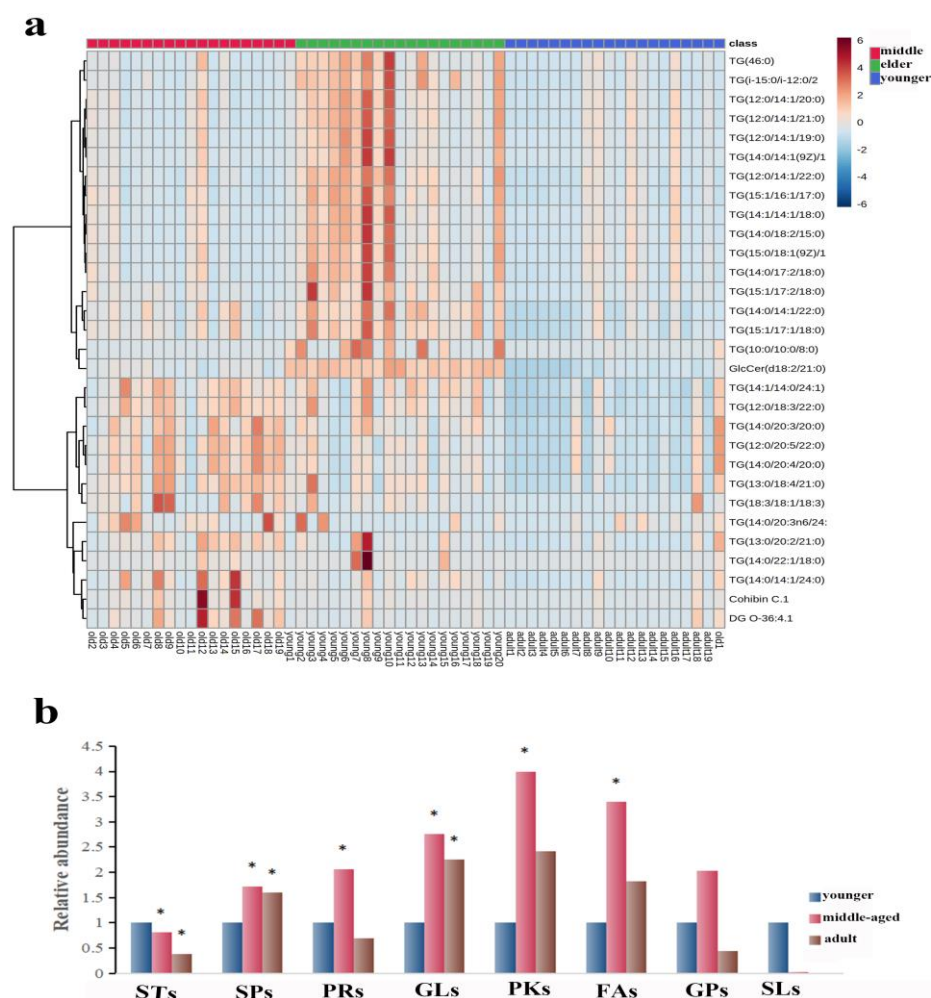


Figure 1. (a): Heatmap illustrating the distribution of SSL among females at different ages. (b): The relative amounts of the eight major lipids in different age groups. The sign of * indicates that the difference is statistically significant when compared with the younger group ($p < 0.05$). Abbreviations: STs, sterol lipids; SPs, sphingolipids; PRs, prenol lipids; GLs, glycerolipids; PKs, polyketides; FAs, fatty acids; GPs, glycerophospholipids; SLs, saccharolipids.

3.2. Multivariate Data Analysis of Right-Hand SSL in Females of Different Age Groups

3.2.1. Sixty-Three Individual Lipids Were Responsible for the Differences between Skin Surface Lipids in Skin Samples

PCA and PLS-DA models were used for multivariate data analysis. The resulting model score plot is shown in Figure 2a,b. These results demonstrated substantial separation and significant differences among the three different age groups of SSL samples ($R_2X = 0.52$, $R_2Y = 0.82$, $Q_2 = 0.56$). According to the loading plot in Figure 2c, after the PCA of the main lipid with a condition of $VIP \geq 1$, the differences among the three groups were further selected. Finally, there were 63 significantly different lipids that were finally identified in Table 2. The selection criteria were $VIP \geq 1$, $p < 0.05$, and fold change > 2 .

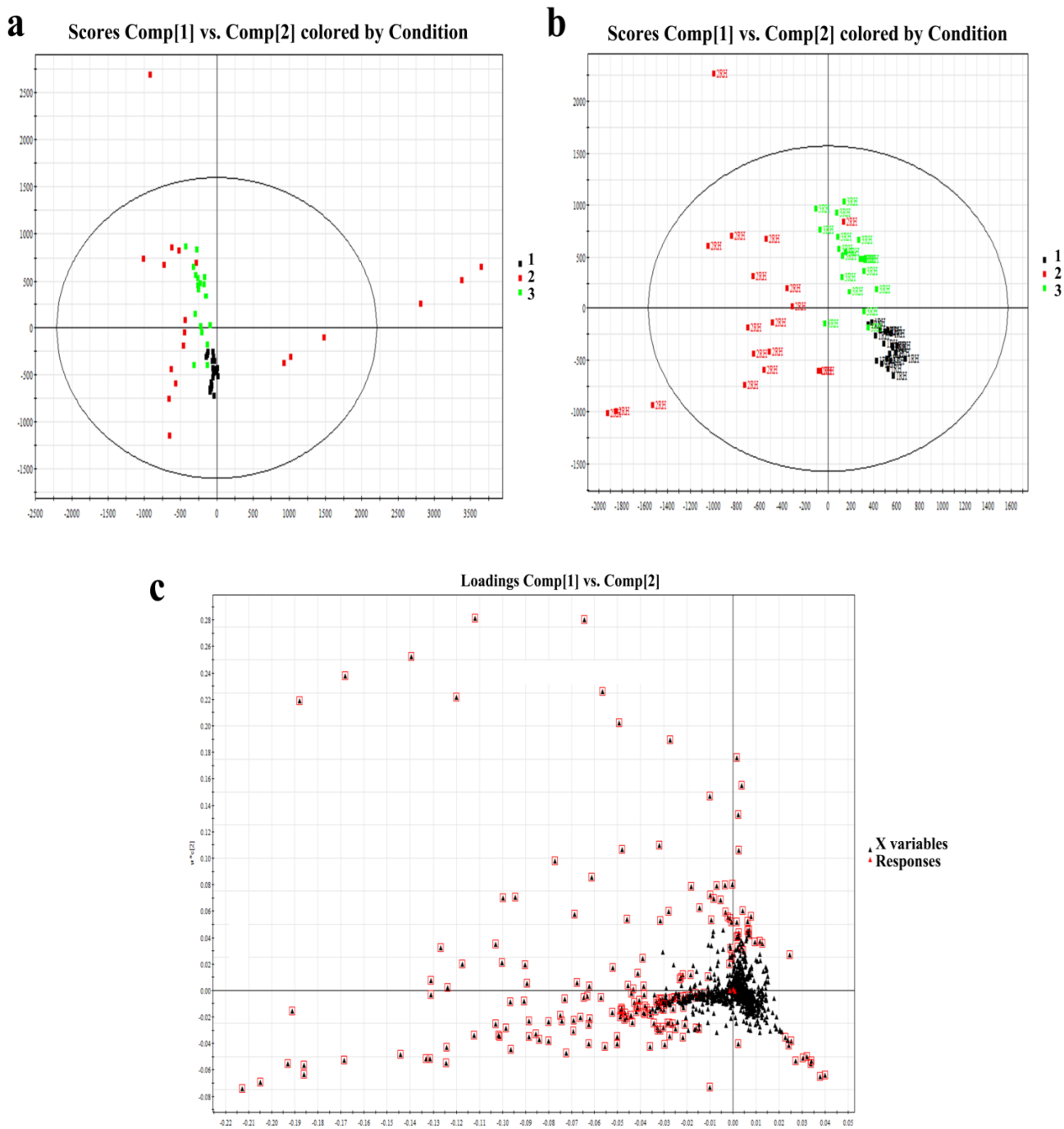


Figure 2. (a): PCA score of right-hand SSL among different-aged females. (b): PLS-DA score of right-hand SSL among different-aged females. RH means right hand. (c): Loading plot of selected components of right-hand SSL among different-aged females in ESI+. Data points marked by red boxes can be seen as the characteristic ions of female SSL in each age group, respectively. 1, younger group; 2, middle-aged group; 3, elder group.

Table 2. The most important individual lipid species responsible for the discrimination between skin surface lipid samples collected from three groups.

Retention Time (min)	<i>m/z</i>	Formula	Description	Anova (<i>p</i>)	Highest Mean
0.8523	262.2384	C ₁₄ H ₂₈ O ₃	3-hydroxy-tetradecanoic acid	0.000	middle-aged
0.8523	218.2124	C ₁₂ H ₂₄ O ₂	FA(12:0)	0.000	middle-aged
1.8561	302.3059	C ₁₈ H ₃₆ O ₂	FA(18:0)	0.000	middle-aged
0.9692	290.2702	C ₁₆ H ₃₂ O ₃	FA(16:0(16-OH))	0.000	middle-aged
0.9692	246.2436	C ₁₄ H ₂₈ O ₂	FA(14:0)	0.000	middle-aged
4.3784	282.2800	C ₁₈ H ₃₂ O	FAL(18:2)	0.000	middle-aged
13.2548	575.5057	C ₃₇ H ₆₆ O ₄	3-(11,12-Dihydroxy-15,19-dotriacontadienyl)-5-methyl-2(5H)-furanone, 9ci	0.000	elder
13.7980	577.5213	C ₃₇ H ₆₈ O ₄	3-[(19Z)-15,16-dihydroxydotriacont-19-en-1-yl]-5-methyl-5H-furan-2-one	0.000	elder
6.6815	355.2852	C ₂₁ H ₃₈ O ₄	MAG(0:0/18:2)	0.000	younger
7.3001	355.2852	C ₂₁ H ₃₈ O ₄	MAG(0:0/18:2n6)	0.000	younger
5.6706	368.4260	C ₂₅ H ₅₀	10Z-Pentacosene	0.002	younger
13.2617	577.5207	C ₃₇ H ₆₈ O ₄	Cohibin C	0.002	elder
5.8905	327.2537	C ₁₉ H ₃₄ O ₄	FA(19:2;O2)	0.006	middle-aged
13.7980	551.5058	C ₃₅ H ₆₆ O ₄	3-(19,20-Dihydroxytriacontyl)-5-methyl-2(5H)-furanone	0.006	elder
1.2578	274.2747	C ₁₆ H ₃₂ O ₂	Diradylglycerols	0.046	middle-aged
1.2509	362.3267	C ₂₀ H ₄₀ O ₄	11,12-dihydroxy arachidic acid	0.048	middle-aged
13.8186	876.8028	C ₅₅ H ₁₀₂ O ₆	TG(14:1/14:0/24:1)	0.000	middle-aged
13.2479	874.7869	C ₅₅ H ₁₀₀ O ₆	TG(12:0/18:3(6Z,9Z,12Z)/22:0)	0.000	elder
14.4376	904.8344	C ₅₇ H ₁₀₆ O ₆	TG(13:0/20:2/21:0)	0.000	elder
12.7256	872.7716	C ₅₅ H ₉₈ O ₆	TG(13:0/18:4/21:0)	0.000	elder
13.2548	900.8024	C ₅₇ H ₁₀₂ O ₆	TG(14:0/20:4/20:0)	0.000	elder
12.7325	881.7627	C ₅₇ H ₁₀₀ O ₆	TG(12:0/20:5/22:0)	0.000	elder
13.8049	603.5368	C ₃₉ H ₇₀ O ₄	DG(O-36:4)	0.000	elder
13.8255	902.8183	C ₅₇ H ₁₀₄ O ₆	TG(14:0/20:3/20:0)	0.000	middle-aged
7.9599	572.4903	C ₃₃ H ₆₂ O ₆	TG(10:0/10:0/10:0)	0.000	younger
14.4376	878.8193	C ₅₅ H ₁₀₄ O ₆	TG(14:0/14:1/24:0)	0.000	elder
7.3070	544.4583	C ₃₁ H ₅₈ O ₆	TG(10:0/10:0/8:0)	0.000	younger
14.4582	956.8639	C ₆₁ H ₁₁₀ O ₆	TG(20:0/20:3/18:1)	0.000	middle-aged
15.7642	960.8970	C ₆₁ H ₁₁₄ O ₆	TG(14:0/20:2/24:0)	0.000	elder
6.1036	488.3956	C ₂₇ H ₅₀ O ₆	TG(8:0/8:0/8:0)	0.001	younger
15.0217	958.8799	C ₆₁ H ₁₁₂ O ₆	TG(14:0/20:3/24:0)	0.001	middle-aged
6.6746	516.4270	C ₂₉ H ₅₄ O ₆	TG(10:0/8:0/8:0)	0.001	younger
15.7504	934.8814	C ₅₉ H ₁₁₂ O ₆	TG(16:0/20:1/20:0)	0.001	elder
12.2370	901.7284	C ₅₉ H ₉₆ O ₆	TG(14:1/20:4/22:4)	0.001	elder
12.7325	903.7431	C ₅₉ H ₉₈ O ₆	TG(16:0/20:4/20:4)	0.001	elder
13.2617	905.7588	C ₅₉ H ₁₀₀ O ₆	TG(16:0/20:4/20:3)	0.001	elder
15.0767	932.8662	C ₅₉ H ₁₁₀ O ₆	TG(14:0/18:2/24:0)	0.002	elder
11.8041	894.7567	C ₅₇ H ₉₆ O ₆	TG(18:3/18:1/18:3)	0.003	elder
15.0905	906.8505	C ₅₇ H ₁₀₈ O ₆	TG(14:0/22:1/18:0)	0.004	elder
13.9492	928.8351	C ₅₉ H ₁₀₆ O ₆	TG(15:0/20:4/21:0)	0.004	elder
14.4720	930.8490	C ₅₉ H ₁₀₈ O ₆	TG(18:0/18:3/20:0)	0.006	elder
12.7187	782.7254	C ₄₈ H ₉₂ O ₆	TG(a-13:0/i-12:0/20:0)	0.009	middle-aged
15.6336	986.9108	C ₆₃ H ₁₁₆ O ₆	TG(22:0/16:1/22:2)	0.009	middle-aged
15.0630	984.8953	C ₆₃ H ₁₁₄ O ₆	TG(20:0/20:0/20:4)	0.017	middle-aged
12.3264	780.7093	C ₄₈ H ₉₀ O ₆	TG(12:0/14:1/19:0)	0.020	middle-aged
12.2714	870.7570	C ₅₅ H ₉₆ O ₆	TG(16:1/20:3/16:1)	0.023	elder
6.6609	516.4614	C ₃₀ H ₅₈ O ₅	DG(8:0/19:0/0:0)	0.039	middle-aged
9.6592	832.2423	C ₃₉ H ₄₃ O ₂₀	Alatanin 2	0.023	middle-aged
8.0079	473.4000	C ₃₁ H ₅₂ O ₃	alpha-Tocopherol acetate	0.000	younger
13.1654	822.8074	C ₅₆ H ₁₀₀ O ₂	alpha-Myrrin cerotate	0.018	middle-aged
8.5101	838.7146	C ₅₀ H ₉₅ NO ₈	Cerebroside	0.000	elder
6.6540	740.6045	C ₄₃ H ₈₁ NO ₈	GlcCer(d15:2(4E,6E)/22:0)	0.000	elder

Table 2. Cont.

Retention Time (min)	<i>m/z</i>	Formula	Description	Anova (<i>p</i>)	Highest Mean
5.4162	413.2673	C ₁₈ H ₃₇ NO ₆ S	Sphing-6E-enine 4R-sufate	0.000	middle-aged
7.3688	522.4893	C ₃₃ H ₆₃ NO ₃	Cer(d18:2/15:0)	0.000	elder
9.7967	678.6408	C ₄₃ H ₈₃ NO ₄	Cer(d18:2/25:0(2OH))	0.000	elder
7.4169	782.6516	C ₄₆ H ₈₇ NO ₈	GlcCer(d18:2/22:0)	0.000	elder
11.9829	948.7871	C ₅₇ H ₁₀₅ NO ₉	Plakoside A	0.000	elder
9.7760	648.6302	C ₄₂ H ₈₁ NO ₃	Cer(D18:1/24:1(15Z))	0.001	elder
9.4457	664.6251	C ₄₂ H ₈₁ NO ₄	Cer(d18:2/24:0(2OH))	0.001	elder
8.0972	750.6111	C ₄₀ H ₈₁ N ₂ O ₇ P	CerPE(d14:1(4E)/24:0(2OH))	0.002	middle-aged
10.4633	676.6615	C ₄₄ H ₈₅ NO ₃	Cer(d18:1/26:1(17Z))	0.003	elder
10.1333	692.6557	C ₄₄ H ₈₅ NO ₄	Cer(d18:2/26:0(2OH))	0.010	elder
21.6564	391.2851	C ₂₄ H ₃₈ O ₄	ST(24:2;O4)	0.000	younger

3.2.2. Classification and Relative Abundance Alterations of Specific Differentiated Lipid Metabolites in Skin Samples

The corresponding metabolites based on the different peaks were divided into six categories through searching the LMSD and HMDB databases, which are presented in Figure 3a. In general, GLs (49.21%), FAs (25.40%), and SPs (19.05%) constituted the majority of the 63 substances. As these classes were predominant among these lipids, we focused on these groups of compounds. In this study, a relative content comparison of these lipid species was analyzed. In Figure 3b, GLs, FAs, and SP levels were lower in the middle-aged group and higher in the elders. It was found that only lower levels of GLs and SPs were statistically significant in the middle-aged group, while higher levels of GLs were found for the elders. Similar observations were made regarding STs and PRs, which seem to be present in the younger group skin (<44 y) and nearly absent in the two older groups combined (>45 y).

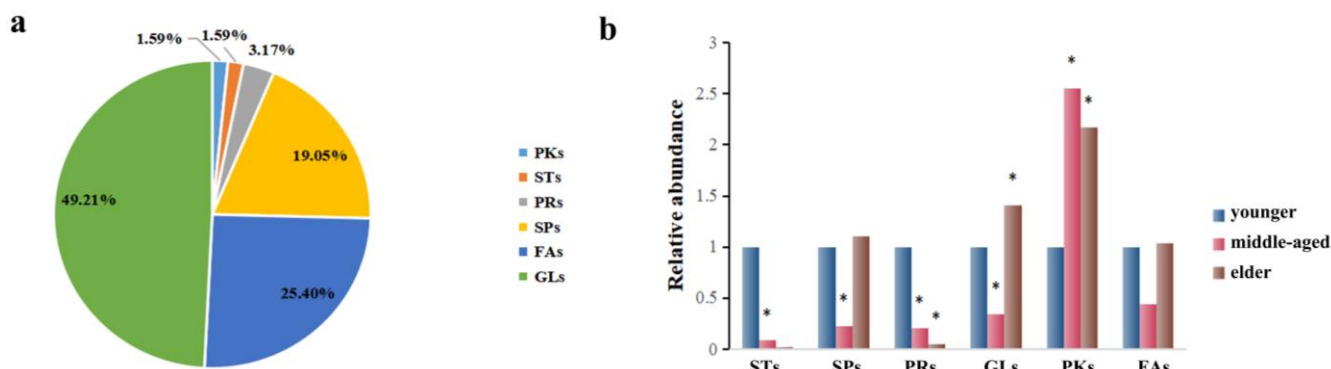


Figure 3. (a): The distribution of the important individual lipid species responsible for the discrimination of samples. (b) Comparison of relative abundance of differentiated metabolites of SSL in different age groups. The sign of * indicates that the difference is statistically significant when compared with the younger group ($p < 0.05$).

The heatmap in Figure 4a shows all the differentiated lipids of the skin samples, and it can clearly be seen that there were differences between the three age groups.

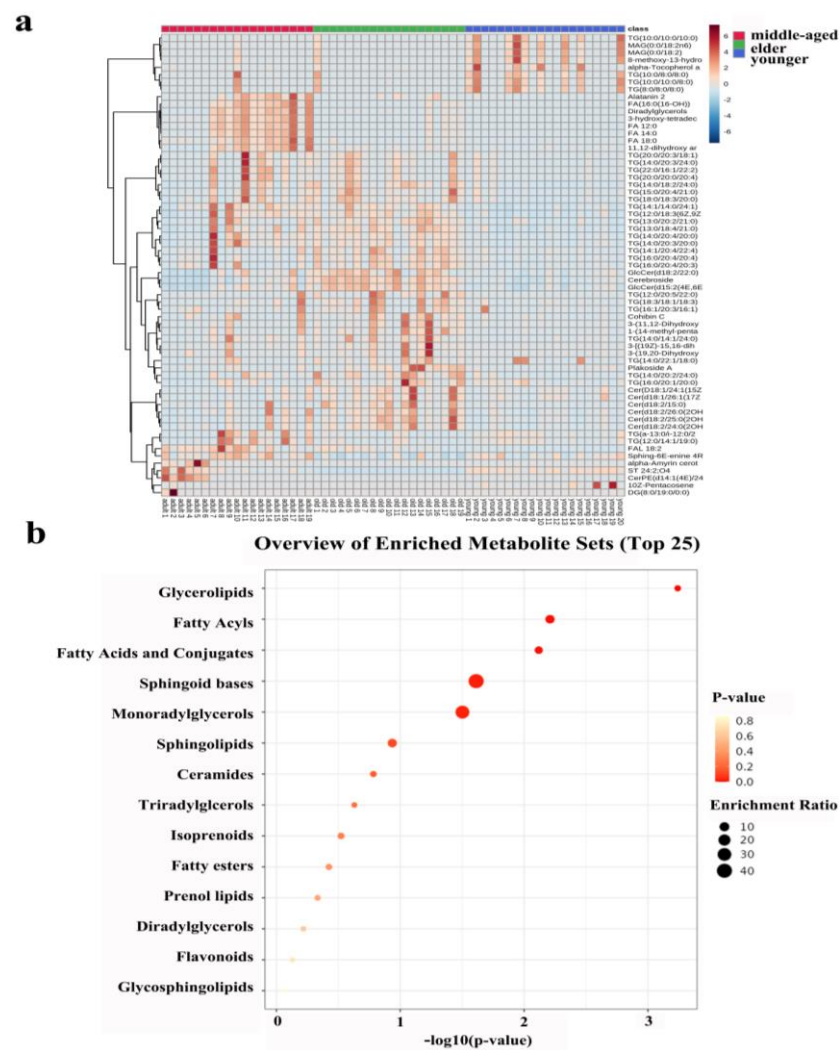


Figure 4. (a): Heatmap illustrating the distribution of SSL among females at different ages. (b): Metabolic pathway of important individual lipids among different age groups.

3.3. Enrichment Analysis of Skin Lipid Metabolism of Right-Hand SSL in Females of Different Age Groups

Lipid metabolism profiles were obtained by the enrichment analysis of SSL in three different age groups of females. Figure 4b showed that the enrichment analysis module identified fourteen kinds of metabolism associated with skin conditions. Obviously, there was no statistical significance for lipid metabolism in the lighter-colored circle at the bottom. From yellow to red, the p -value is from large to small, indicating that the degree of enrichment is becoming more and more significant. There are lipid pathways on the vertical axis and enrichment factors on the horizontal axis; the higher the value, the greater the degree of enrichment. The size of the dots represents the number of lipids enriched in this pathway. Our results showed that the most statistically significant and largest enrichment lipid metabolism was GLs. In addition, the lipid individuals enriched to the sphingoid bases metabolism were the most and statistically significant.

4. Discussion

Focusing on the status of skin in different life courses, we describe the application of UPLC-QTOF-MS-based lipidomics in the study of SSL differences in different age groups. This approach provides comprehensive information on the mechanisms underlying differences in skin status across ages. In our study, we validated the differences in SSL in different age groups through lipidomic models. By searching the database, the differenti-

ated metabolites were classified and compared according to their relative abundance to try to obtain the change in skin lipids at different ages.

Overall, we identified a total of 530 lipids and observed that, among the eight main classes of lipids, the pattern of expression of GLs and SPs seems to indicate that the younger group (<44 y) expresses fewer of these lipid types than the two older groups combined (>45 y). After statistical processing, it was found that surface skin differential lipids were mainly concentrated in FAs, GLs, and SPs. The levels of GLs, FAs, and SP among females in the middle-aged group were lower than those of younger females, while the levels were higher among elders. However, there was only a statistically significant difference between lower levels of GLs and SPs in the middle-aged group and the higher levels of GLs in the elder group. In addition, similar observations have been made regarding STs and PRs. These seem to be present in the younger group skin and nearly absent in the two older groups together. It would be interesting to identify several representative lipids that can be used as examples for these lipid families.

As the research progressed, techniques such as the analysis of stratum corneum lipid components, including tape stripping, and corneal surface measurement were being used to measure the effects of interventions on (elderly) skin and 3D organ models [23]. It has been confirmed that both intrinsic and extrinsic aging have an effect on the morphology of corneal cells, with the surface area increasing or decreasing [24]. One study using scanning electron microscopy found that two opposing aging effects resulted in no significant differences in physical aging between hand samples from two age groups [25]. Unlike internally aging skin, external aging (UV irradiation) is manifested by thickening of the epidermis, especially the stratum corneum, which disrupts the western differentiation of keratin [26,27]. Furthermore, changes in transepidermal water loss are observed to be an acute stress response under the action of external aging factors such as ultraviolet radiation [28]. In addition to specific changes in skin appearance and function, the lipid processing of keratinocytes declines with age. This causes quantitative and qualitative changes in lipophilic molecules within the SC membrane [29].

The skin plays an important role as a barrier between the harsh external environment and the host. Certainly, the two barriers are essential for survival: the barrier to water and electrolytes (osmotic barrier) as well as the barrier to invading and toxic microorganisms (antibacterial barrier). Lipids play a crucial role in the formation and maintenance of these barriers [30]. The hydrophobic extracellular lipid matrix in the stratum corneum is mainly composed of Cers, cholesterol, and free FAs, providing a barrier to the movement of water and electrolytes [31]. A variety of lipids, such as FAs, monoglycerides, SPs, phospholipids, and especially FAs, have antibacterial activity and contribute to the formation of antibacterial barriers [32].

As a type of lipid on the surface of the skin, FAs is an important ingredient that maintains the function of the skin barrier. Symptoms of FAs deficiency include dryness of the epidermis, peeling, loose skin, skin inflammation, increased sensitivity to irritation, and slow healing [33]. A recent study of FAs in the skin epidermis found an age-dependent content of the major lipid components, with the main difference being the level of polyunsaturated fatty acids [34]. This is different from our finding that the differential fatty acids are saturated fatty acids such as stearic acid and palmitic acid. It is interesting to note that, unlike C15:0 and C17:0, which were shown in a study on aging to decrease in FAs on the skin's surface [35], our study was screened to find that the age difference was mostly an even number of long-chain FAs. Previous studies have shown that free FAs present in sebum (such as lauric acid C12:0, palmitic acid C16:0, and oleic acid C18:0) can induce sebaceous cells to express antimicrobial peptides, affecting the inflammatory and antibacterial processes of the skin [36]. FAs derived from fish oil are thought to be involved in skin photoprotection [36]. Other mechanisms by which omega-3 PUFAs inhibit UV-induced keratinocyte damage may be the modulation of COX-2, NF- κ b, and mitogen-activated protein kinase (MAPK)/extracellular signal-regulated kinase (ERK) pathways [37]. According to the results of this study, among females, the level of FAs on the surface of the

right-hand skin was lower in the middle-aged group compared to the younger group. The overall condition of the skin—its surface texture, color, and physiological properties—is determined by factors such as hydration (i.e., a sufficient amount of water in the stratum corneum), sebum content, and surface acidity. Middle-aged women, especially in rural areas, are basically inseparable from housework; thus, inevitably, they undergo long-term exposure to various detergents. After detergent exposure, not only is the PH of the skin affected [38], but the FAs content of the skin also changes. Compared with those before exposure, after exposure, the long-chain FAs are reduced, the density of the lipid tissue is lower, and the layered structure of the extracellular stratum cornea is changed, resulting in skin barrier dysfunction [39,40].

Decreased levels of free FAs and triglycerides in the SC of aging skin are consistent with previous studies [41]. These skin lipid reductions may be caused by UV exposure affecting the activity of several cytokines. These cytokines include interleukin (IL)-6, IL-8, placental growth factor, and C-C base multiplex chemokines (CCL)2/MCP-3 produced by ultraviolet irradiation on keratinocytes or fibroblasts [42]. As previous studies have shown, the difference in lipid levels and lipatopoietic enzymes in SC fat in light-damaged forearm skin and light-protected buttock skin is not due to differences in anatomical location but rather due to the effects of ultraviolet radiation [43]. One study suggests that age-dependent adaptation of the upper glycolysis and glycerol metabolism interface has a potential effect on epidermal barrier function [44]. This decrease in glycerol metabolism can have serious consequences for the lipid layer of the cuticle epidermal barrier and may lead to the impaired barrier function of aging skin [45]. In one study simulating UV irradiation, the most significant lipid changes were found to be increases in long-chain Cers, LysoPC, and glycerides, while phospholipids such as phosphatidylcholine (PC) and phosphatidylethanolamine (PE) did not follow a clear increase/decrease pattern [46]. Similarly, one Japanese study found a trend toward decreased skin ceramide and cholesterol in older adults. The skin is the target organ for hormones [47]. Ovarian estrogen, which accounts for the majority of estrogen in women, declines with age, especially during menopause. Postmenopausal estrogen deficiency can lead to skin atrophy and accelerate skin aging [48]. Early studies have shown that sterols are closely related to skin conditions, such as acne [49,50]. Recent studies also suggested that the majority of differentiating lipid species were diacylglycerols (DGs), followed by fatty acyls, sterols, and prenols, which are more abundant in the skin of acne patients [51]. To our knowledge, no studies have explored the association between age and sterols and PRs [52].

A previous study using time-of-flight secondary ion mass spectrometry to examine age-related changes in human stratum corneum lipids found significant age-related increases and changes in the spatial distribution of sterol-cholesterol sulfate, a membrane-stable lipid [25]. However, in our study, no differences in this substance were found between different age groups. Our results suggest that sphingoid bases may suggest a novel age-related metabolic pathway. Sphingomyelins are a class of lipids that contain long-chain (C16-C20) amino alcohols (sphingosine bases). As the backbone structure of all SPs (i.e., schingolipids and phospholipids), Cers are metabolites including sphingosine bases, sphingosine-1-phosphate, and Cers-1-phosphate [53]. Sphingosine regulates cellular function by sphingosine kinase (sphk1 and sphk2) 1-phosphate (S1P), which is synthesized by sphingosine and by S1P receptor-dependent and non-dependent pathways. It has been found that sphingosine groups can be used in conjunction with other lipids as biomarkers for FAs to predict atopic dermatitis in children [54]. Meanwhile, a large number of studies have shown that the pharmacological regulation of Cers and sphingosines in the skin helps to treat skin diseases associated with the abnormal proliferation and differentiation of the epidermis and inflammation [55].

Aging is a complex and variable process, which is difficult to quantify and interpret. This study used lipidomics to explore the mechanism of skin barrier function damage with age, quantify the degree of damage, and find important related lipid metabolism, which provides a theoretical basis for the development and optimization of corresponding

anti-aging hand skincare products. Moreover, the study of aging from the perspective of lipids provides a scientific basis for the development of geriatric dermatology. This will enable us to further guide clinical medication and the prevention of skin diseases. However, due to the limitations of observational studies, more in-depth mechanistic studies determining whether the observed effects on the metabolites reported are due to epigenetic regulation will be performed in our future studies.

5. Conclusions

There were differences in the right-hand SSL of females at different ages, and the differences may be related to the metabolism of GLs and sphingoid bases.

Supplementary Materials: The following supporting information can be downloaded at: <https://www.mdpi.com/article/10.3390/metabo13040553/s1>, Table S1: The detailed ion source conditions of quadrupole time-of-flight mass spectrometry.

Author Contributions: All authors contributed to the study conduct/data collection. T.C. and Z.M. designed the research; T.C. analyzed the data and drafted the manuscript; Z.M. and J.W. commented on previous versions of the manuscript. All authors have read and agreed to the published version of the manuscript.

Funding: This research received no external funding.

Institutional Review Board Statement: This study conforms to the principles of the Declaration of Helsinki, was registered in the China Clinical Trial Center (ID: ChiCTR2000034103), and was conducted with the approval of the Ethics Committee of Zhengzhou University.

Informed Consent Statement: Informed consent was obtained from all subjects involved in the study.

Data Availability Statement: The data presented in this study are available in article and supplementary material.

Acknowledgments: The authors thank the participants, coordinators, and administrators for their support and the laboratory at the school of Public Health Zhengzhou University for the facility support during the study. The authors thank Guo Yiguang of the Research Center of Yuze Skin Health for his support.

Conflicts of Interest: The authors declare that they have no known competing financial interests or personal relationships that could have appeared to influence the work reported in this paper.

References

1. Clark, R.A.; Ghosh, K.; Tonnesen, M.G. Tissue engineering for cutaneous wounds. *J. Investig. Dermatol.* **2007**, *127*, 1018–1029. [[CrossRef](#)] [[PubMed](#)]
2. Miao, Q.; Hill, M.C.; Chen, F.; Mo, Q.; Ku, A.T.; Ramos, C.; Sock, E.; Lefebvre, V.; Nguyen, H. SOX11 and SOX4 drive the reactivation of an embryonic gene program during murine wound repair. *Nat. Commun.* **2019**, *10*, 4042. [[CrossRef](#)]
3. Breiden, B.; Sandhoff, K. The role of sphingolipid metabolism in cutaneous permeability barrier formation. *Biochim. Et Biophys. Acta* **2014**, *1841*, 441–452. [[CrossRef](#)]
4. Morelli, P.; Gaspari, M.; Gabriele, C.; Dastoli, S.; Bennardo, L.; Pavel, A.B.; Patruno, C.; Del Duca, E.; Nisticò, S.P. Proteomic analysis from skin swabs reveals a new set of proteins identifying skin impairment in atopic dermatitis. *Exp. Dermatol.* **2021**, *30*, 811–819. [[CrossRef](#)]
5. Hänel, K.H.; Cornelissen, C.; Lüscher, B.; Baron, J.M. Cytokines and the skin barrier. *Int. J. Mol. Sci.* **2013**, *14*, 6720–6745. [[CrossRef](#)]
6. Feingold, K.R. Lamellar bodies: The key to cutaneous barrier function. *J. Investig. Dermatol.* **2012**, *132*, 1951–1953. [[CrossRef](#)]
7. Hadgraft, J.; Lane, M.E. Transepidermal water loss and skin site: A hypothesis. *Int. J. Pharm.* **2009**, *373*, 1–3. [[CrossRef](#)] [[PubMed](#)]
8. Biniek, K.; Kaczvinsky, J.; Matts, P.; Dauskardt, R.H. Understanding age-induced alterations to the biomechanical barrier function of human stratum corneum. *J. Dermatol. Sci.* **2015**, *80*, 94–101. [[CrossRef](#)]
9. Rittié, L.; Fisher, G.J. Natural and sun-induced aging of human skin. *Cold Spring Harb. Perspect. Med.* **2015**, *5*, a015370. [[CrossRef](#)]
10. Chalyk, N.E.; Bandaletova, T.Y.; Kyle, N.H.; Petyaev, I.M. Morphological Characteristics of Residual Skin Surface Components Collected from the Surface of Facial Skin in Women of Different Age. *Ann. Dermatol.* **2017**, *29*, 454–461. [[CrossRef](#)] [[PubMed](#)]
11. Bize, C.; Le Gélébart, E.; Moga, A.; Payré, B.; Garcia, C. Barrier disruption, dehydration and inflammation: Investigation of the vicious circle underlying dry skin. *Int. J. Cosmet. Sci.* **2021**, *43*, 729–737. [[CrossRef](#)] [[PubMed](#)]
12. Langan, S.M.; Irvine, A.D.; Weidinger, S. Atopic dermatitis. *Lancet* **2020**, *396*, 345–360. [[CrossRef](#)] [[PubMed](#)]

13. Han, X. Lipidomics for studying metabolism. *Nat. Rev. Endocrinol.* **2016**, *12*, 668–679. [[CrossRef](#)] [[PubMed](#)]
14. Li, H.; Ning, S.; Ghandi, M.; Kryukov, G.V.; Gopal, S.; Deik, A.; Souza, A.; Pierce, K.; Keskula, P.; Hernandez, D.; et al. The landscape of cancer cell line metabolism. *Nat. Med.* **2019**, *25*, 850–860. [[CrossRef](#)]
15. Chatelaine, H.; Dey, P.; Mo, X.; Mah, E.; Bruno, R.S.; Kopec, R.E. Vitamin A and D Absorption in Adults with Metabolic Syndrome versus Healthy Controls: A Pilot Study Utilizing Targeted and Untargeted LC-MS Lipidomics. *Mol. Nutr. Food Res.* **2021**, *65*, e2000413. [[CrossRef](#)]
16. Sobolev, V.V.; Mezentsev, A.V.; Ziganshin, R.H.; Soboleva, A.G.; Denieva, M.; Korsunskaya, I.M.; Svitich, O.A. LC-MS/MS analysis of lesional and normally looking psoriatic skin reveals significant changes in protein metabolism and RNA processing. *PLoS ONE* **2021**, *16*, e240956. [[CrossRef](#)]
17. Jeong, H.; Kim, S.; Seo, Y.; Koh, J.; Baek, J. Investigation of symptoms of hand skin changes with aging in Korean women and development of a new standard grading scale for hand aging. *Ski. Res. Technol. Off. J. Int. Soc. Bioeng. Ski.* **2020**, *26*, 788–793. [[CrossRef](#)]
18. Carmeli, E.; Patish, H.; Coleman, R. The aging hand. *J. Gerontol. Ser. A Biol. Sci. Med. Sci.* **2003**, *58*, 146–152. [[CrossRef](#)]
19. Shetage, S.S.; Traynor, M.J.; Brown, M.B.; Chilcott, R.P. Sebomic identification of sex- and ethnicity-specific variations in residual skin surface components (RSSC) for bio-monitoring or forensic applications. *Lipids Health Dis.* **2018**, *17*, 194. [[CrossRef](#)]
20. Xian, M.; Wawrzyniak, P.; Rückert, B.; Duan, S.; Meng, Y.; Sokolowska, M.; Globinska, A.; Zhang, L.; Akdis, M.; Akdis, C.A. Anionic surfactants and commercial detergents decrease tight junction barrier integrity in human keratinocytes. *J. Allergy Clin. Immunol.* **2016**, *138*, 890–893.e899. [[CrossRef](#)]
21. Li, M.; Vierkötter, A.; Schikowski, T.; Hüls, A.; Ding, A.; Matsui, M.S.; Deng, B.; Ma, C.; Ren, A.; Zhang, J.; et al. Epidemiological evidence that indoor air pollution from cooking with solid fuels accelerates skin aging in Chinese women. *J. Dermatol. Sci.* **2015**, *79*, 148–154. [[CrossRef](#)] [[PubMed](#)]
22. Zhou, Y.; Guo, S.; He, Y.; Zuo, Q.; Liu, D.; Xiao, M.; Fan, J.; Li, X. COVID-19 Is Distinct From SARS-CoV-2-Negative Community-Acquired Pneumonia. *Front. Cell. Infect. Microbiol.* **2020**, *10*, 322. [[CrossRef](#)]
23. Alexander, L.; Wood, C.M.; Gaskin, P.L.R.; Sawiak, S.J.; Fryer, T.D.; Hong, Y.T.; McIver, L.; Clarke, H.F.; Roberts, A.C. Over-activation of primate subgenual cingulate cortex enhances the cardiovascular, behavioral and neural responses to threat. *Nat. Commun.* **2020**, *11*, 5386. [[CrossRef](#)]
24. Huang, J.; Heng, S.; Zhang, W.; Liu, Y.; Xia, T.; Ji, C.; Zhang, L.J. Dermal extracellular matrix molecules in skin development, homeostasis, wound regeneration and diseases. *Semin. Cell Dev. Biol.* **2022**, *128*, 137–144. [[CrossRef](#)]
25. Starr, N.J.; Johnson, D.J.; Wibawa, J.; Marlow, I.; Bell, M.; Barrett, D.A.; Scurr, D.J. Age-Related Changes to Human Stratum Corneum Lipids Detected Using Time-of-Flight Secondary Ion Mass Spectrometry Following in Vivo Sampling. *Anal. Chem.* **2016**, *88*, 4400–4408. [[CrossRef](#)] [[PubMed](#)]
26. Zorina, A.; Zorin, V.; Kudlay, D.; Kopnin, P. Molecular Mechanisms of Changes in Homeostasis of the Dermal Extracellular Matrix: Both Involutional and Mediated by Ultraviolet Radiation. *Int. J. Mol. Sci.* **2022**, *23*, 6655. [[CrossRef](#)] [[PubMed](#)]
27. D’Orazio, J.; Jarrett, S.; Amaro-Ortiz, A.; Scott, T. UV radiation and the skin. *Int. J. Mol. Sci.* **2013**, *14*, 12222–12248. [[CrossRef](#)]
28. Low, E.; Alimohammadiha, G.; Smith, L.A.; Costello, L.F.; Przyborski, S.A.; von Zglinicki, T.; Miwa, S. How good is the evidence that cellular senescence causes skin ageing? *Ageing Res. Rev.* **2021**, *71*, 101456. [[CrossRef](#)]
29. Jia, Y.; Gan, Y.; He, C.; Chen, Z.; Zhou, C. The mechanism of skin lipids influencing skin status. *J. Dermatol. Sci.* **2018**, *89*, 112–119. [[CrossRef](#)]
30. de Szalay, S.; Wertz, P.W. Protective Barriers Provided by the Epidermis. *Int. J. Mol. Sci.* **2023**, *24*, 3145. [[CrossRef](#)]
31. Feingold, K.R. Thematic review series: Skin lipids. The role of epidermal lipids in cutaneous permeability barrier homeostasis. *J. Lipid Res.* **2007**, *48*, 2531–2546. [[CrossRef](#)]
32. Elias, P.M. The skin barrier as an innate immune element. *Semin. Immunopathol.* **2007**, *29*, 3–14. [[CrossRef](#)] [[PubMed](#)]
33. Wohlrab, J.; Gabel, A.; Wolfram, M.; Grosse, I.; Neubert, R.H.H.; Steinbach, S.C. Age- and Diabetes-Related Changes in the Free Fatty Acid Composition of the Human Stratum Corneum. *Ski. Pharmacol. Physiol.* **2018**, *31*, 283–291. [[CrossRef](#)] [[PubMed](#)]
34. Mika, A.; Pakiet, A.; Szczygielski, O.; Woźniak, K.; Osipowicz, K.; Kowalewski, C.; Krześniak, N.; Noszczyk, B.H.; Wertheim-Tysarowska, K. Fatty acid profiles in various lipid fractions in the female epidermis. Does the body site and age matter? *Acta Biochim. Pol.* **2022**, *69*, 657–671. [[CrossRef](#)]
35. Sanford, J.A.; O’Neill, A.M.; Zouboulis, C.C.; Gallo, R.L. Short-Chain Fatty Acids from *Cutibacterium acnes* Activate Both a Canonical and Epigenetic Inflammatory Response in Human Sebocytes. *J. Immunol.* **2019**, *202*, 1767–1776. [[CrossRef](#)]
36. Pilkington, S.M.; Watson, R.E.; Nicolaou, A.; Rhodes, L.E. Omega-3 polyunsaturated fatty acids: Photoprotective macronutrients. *Exp. Dermatol.* **2011**, *20*, 537–543. [[CrossRef](#)] [[PubMed](#)]
37. Chiang, H.M.; Chan, S.Y.; Chu, Y.; Wen, K.C. Fisetin Ameliorated Photodamage by Suppressing the Mitogen-Activated Protein Kinase/Matrix Metalloproteinase Pathway and Nuclear Factor- κ B Pathways. *J. Agric. Food Chem.* **2015**, *63*, 4551–4560. [[CrossRef](#)]
38. Nováčková, A.; Sagrafena, I.; Pullmannová, P.; Paraskevopoulos, G.; Dwivedi, A.; Mazumder, A.; Růžicková, K.; Slepíčka, P.; Zbytovská, J.; Vávrová, K. Acidic pH Is Required for the Multilamellar Assembly of Skin Barrier Lipids In Vitro. *J. Investig. Dermatol.* **2021**, *141*, 1915–1921.e1914. [[CrossRef](#)] [[PubMed](#)]
39. Lima, A.L.; Timmermann, V.; Illing, T.; Elsner, P. Contact Dermatitis in the Elderly: Predisposing Factors, Diagnosis, and Management. *Drugs Aging* **2019**, *36*, 411–417. [[CrossRef](#)]

40. Lodén, M.; Bárány, E. Skin-identical lipids versus petrolatum in the treatment of tape-stripped and detergent-perturbed human skin. *Acta Derm. Venereol.* **2000**, *80*, 412–415. [[CrossRef](#)] [[PubMed](#)]
41. Kim, E.J.; Kim, Y.K.; Kim, S.; Kim, J.E.; Tian, Y.D.; Doh, E.J.; Lee, D.H.; Chung, J.H. Adipochemokines induced by ultraviolet irradiation contribute to impaired fat metabolism in subcutaneous fat cells. *Br. J. Dermatol.* **2018**, *178*, 492–501. [[CrossRef](#)]
42. Li, W.H.; Pappas, A.; Zhang, L.; Ruvolo, E.; Cavender, D. IL-11, IL-1 α , IL-6, and TNF- α are induced by solar radiation in vitro and may be involved in facial subcutaneous fat loss in vivo. *J. Dermatol. Sci.* **2013**, *71*, 58–66. [[CrossRef](#)]
43. Kim, E.J.; Kim, Y.K.; Kim, J.E.; Kim, S.; Kim, M.K.; Park, C.H.; Chung, J.H. UV modulation of subcutaneous fat metabolism. *J. Investig. Dermatol.* **2011**, *131*, 1720–1726. [[CrossRef](#)]
44. Kuehne, A.; Hildebrand, J.; Soehle, J.; Wenck, H.; Terstegen, L.; Gallinat, S.; Knott, A.; Winnefeld, M.; Zamboni, N. An integrative metabolomics and transcriptomics study to identify metabolic alterations in aged skin of humans in vivo. *BMC Genom.* **2017**, *18*, 169. [[CrossRef](#)]
45. Martin, R.P.; Varela, P.; Gomes, C.P.; Marins, M.M.; Filippelli-Silva, R.; Yarak, S.; Soares, J.L.M.; Sanudo, A.; Idkowiak-Baldys, J.; Chen, S.; et al. Transcriptomic and histological analysis of exposed facial skin areas wrinkled or not and unexposed skin. *Mol. Biol. Rep.* **2022**, *49*, 1669–1678. [[CrossRef](#)]
46. Dalmau, N.; Andrieu-Abadie, N.; Tauler, R.; Bedia, C. Phenotypic and lipidomic characterization of primary human epidermal keratinocytes exposed to simulated solar UV radiation. *J. Dermatol. Sci.* **2018**, *92*, 97–105. [[CrossRef](#)]
47. Egawa, M.; Tagami, H. Comparison of the depth profiles of water and water-binding substances in the stratum corneum determined in vivo by Raman spectroscopy between the cheek and volar forearm skin: Effects of age, seasonal changes and artificial forced hydration. *Br. J. Dermatol.* **2008**, *158*, 251–260. [[CrossRef](#)] [[PubMed](#)]
48. Liu, T.; Li, N.; Yan, Y.Q.; Liu, Y.; Xiong, K.; Liu, Y.; Xia, Q.M.; Zhang, H.; Liu, Z.D. Recent advances in the anti-aging effects of phytoestrogens on collagen, water content, and oxidative stress. *Phytother. Res. PTR* **2020**, *34*, 435–447. [[CrossRef](#)]
49. Bedord, C.J.; Young, J.M. A comparison of comedonal and skin surface lipids from hairless dogs showing clinical signs of acne. *J. Investig. Dermatol.* **1981**, *77*, 341–344. [[CrossRef](#)]
50. Lasch, J.; Schönfelder, U.; Walke, M.; Zellmer, S.; Beckert, D. Oxidative damage of human skin lipids. Dependence of lipid peroxidation on sterol concentration. *Biochim. Et Biophys. Acta* **1997**, *1349*, 171–181. [[CrossRef](#)] [[PubMed](#)]
51. Camera, E.; Ludovici, M.; Tortorella, S.; Sinagra, J.L.; Capitanio, B.; Goracci, L.; Picardo, M. Use of lipidomics to investigate sebum dysfunction in juvenile acne. *J. Lipid Res.* **2016**, *57*, 1051–1058. [[CrossRef](#)]
52. Misawa, E.; Tanaka, M.; Saito, M.; Nabeshima, K.; Yao, R.; Yamauchi, K.; Abe, F.; Yamamoto, Y.; Furukawa, F. Protective effects of Aloe sterols against UVB-induced photoaging in hairless mice. *Photodermatol. Photoimmunol. Photomed.* **2017**, *33*, 101–111. [[CrossRef](#)]
53. Nojiri, K.; Fudetani, S.; Arai, A.; Kitamura, T.; Sassa, T.; Kihara, A. Impaired Skin Barrier Function Due to Reduced ω -O-Acylceramide Levels in a Mouse Model of Sjögren-Larsson Syndrome. *Mol. Cell. Biol.* **2021**, *41*, e0035221. [[CrossRef](#)] [[PubMed](#)]
54. Rinnov, M.R.; Halling, A.S.; Gerner, T.; Ravn, N.H.; Knudgaard, M.H.; Trautner, S.; Goorden, S.M.I.; Ghauharali-van der Vlugt, K.J.M.; Stet, F.S.; Skov, L.; et al. Skin biomarkers predict development of atopic dermatitis in infancy. *Allergy* **2022**, *78*, 791–802. [[CrossRef](#)]
55. Toncic, R.J.; Jakasa, I.; Hadzavdic, S.L.; Goorden, S.M.; Vlugt, K.J.G.; Stet, F.S.; Balic, A.; Petkovic, M.; Pavicic, B.; Zuzul, K.; et al. Altered Levels of Sphingosine, Sphinganine and Their Ceramides in Atopic Dermatitis Are Related to Skin Barrier Function, Disease Severity and Local Cytokine Milieu. *Int. J. Mol. Sci.* **2020**, *21*, 1958. [[CrossRef](#)]

Disclaimer/Publisher’s Note: The statements, opinions and data contained in all publications are solely those of the individual author(s) and contributor(s) and not of MDPI and/or the editor(s). MDPI and/or the editor(s) disclaim responsibility for any injury to people or property resulting from any ideas, methods, instructions or products referred to in the content.